Appl. Phys. B 92, 13–18 (2008)
DOI: 10.1007/s00340-008-3058-7

Applied Physics B
Lasers and Optics

W.-Y. CHENG✉
T.-H. WU
S.-W. HUANG
S.-Y. LIN
C.-M. WU

Stabilizing the frequency of femtosecond Ti:sapphire comb laser by a novel scheme

IAMS, Institute of Atomic and Molecular Science, Academia Sinica, Taiwan, R.O.C.

Received: 31 March 2008/Revised version: 22 April 2008
Published online: 12 June 2008 •

ABSTRACT We demonstrated a novel scheme for scanning the absolute frequencies of a femtosecond Kerr-lens mode-locked Ti:sapphire laser with the repetition rate unaffected, where the carrier-envelop phase of the pulse was controlled by slightly shifting pump beam and the repetition rate was phase locked to a stable radio-frequency oscillator. Since it was the first time to stabilize the frequency of a mode-locked laser by referring directly to the frequency of cesium two-photon-transition (TPT) stabilized diode laser, we evaluated the frequency instability and the frequency accuracy that showed the characteristic of being a comb laser. The feature of the comb laser in this report will be significant for multi-photon spectroscopy where the frequency difference between comb lines plays a key role.

PACS 06.30.+v; 42.60.By

1 Introduction

Femtosecond mode-locked lasers, also called "optical frequency comb lasers" whenever their absolute frequencies were stabilized, have recently been shown to be novel light sources in the aspect of light–matter interaction. For instance, scientists have used frequency-stabilized mode-locked lasers to demonstrate quantum interference [1], control atomic excited state population [2] and perform wide-band high-resolution molecular spectroscopy [3, 4]. In the past, people stabilized the absolute frequencies of mode-locked lasers by the scheme of so-called "self-reference" [5, 6], or by the scheme of referring to wavelength standard lasers [7, 8], in that spectrum expansion by mode-locked lasers or step-wise phase-locking by frequency chain were usually required. In this paper we showed, by evaluating the frequency accuracy, that the frequency of atomic cesium $6s \to 8s$ two-photon transition (TPT) stabilized diode laser could be a good frequency reference of Ti:sapphire comb laser; neither microstructure fiber nor a frequency chain was needed. The absolute comb frequency locking was realized by controlling the horizontal shift of the pump beam and the repetition rate was phase-locked to a stable radio frequency. The advantage of this approach is that orthogonal control between repetition rate (f_{rep}) and absolute frequency (f_n) could be easily reached, which benefits for the experiments of multi-photon spectroscopy where repetition rate plays key role, such as the phenomenon of coherent population trapping (CPT). Furthermore, the approach of the shifting pump beam enlarges the frequency capture range to one order of magnitude comparing with that by varying the pump power [9, 10]. Our approach on building up the comb laser can spare more than 99% available comb laser power for applications since only 3 mW comb laser power was needed for the absolute frequency locking. This is particularly advantageous for some experiments, such as nonlinear laser spectroscopy [1, 11, 12] by comb laser, that needs higher comb laser power. however, it was known that comb laser frequencies were very sensitive to the variation of repetition rate (f_{rep}) whereas the f_{rep} drift was inevitable. We overcome this problem by designing a particular cooling base and the free drift of f_{rep} was successfully controlled within 50 Hz so that the general problem of long-tern f_{rep}-drift of Ti:sapphire laser systems was resolved.

In terms of direct frequency locking, other researchers have directly locked the frequency of a mode-locked Ti:sapphire laser against a wide-band coating Fabry–Pérot cavity [13]. However, reliable atomic or molecular references were always needed to ensure the reproducibility of absolute frequencies. Hence, we chose a narrow resonance of atomic cesium $6S_{1/2} \to 8S_{1/2}$ ($F = 3 \to F = 3$) hyperfine transition (TPT, 822 nm) as the reliable reference of our pulse laser. The advantages are;

1. The transition frequency has been determined [11].
2. The corresponding diode laser (822 nm) is commercially available that adds the flexibility to integrate this frequency reference laser into optical systems.
3. The transition wavelength is within the gain center of Ti:sapphire laser emission spectrum. Therefore, neither expanding comb laser spectrum nor setting up frequency chain is needed to lock pulse frequencies.
4. The $S \to S$ hyperfine transitions are free from linear Zeeman shift that keeps comb frequencies in good reproducibility.
5. The corresponding hyperfine transitions ($F = 3 \to F = 3$ and $F = 4 \to F = 4$), with their high spectral separation (> 4 GHz), could be easily identified by a commercial wave meter.

✉ Fax: +886-2-23624944, E-mail: wycheng@gate.sinica.edu.tw

2 Setup

2.1 *Outlook*

Figure 1 is the block diagram of our experimental setup. The reliable frequency reference of pulse laser was provided by a cesium two-photon stabilized (CTS) diode laser system, with a 4.4×10^{-13} ($\Delta f = 160$ Hz at 60 s) frequency instability [14]. The double-pass acoustic-optical modulator (DPA) is for modulating laser frequency to retrieve the cesium TPT hyperfine spectrum, and for linearly scanning the absolute frequency of pulse laser that will be mentioned in details in Sect. 2.3. A stray light from the wedged output coupler of a Kerr-lens mode-locked (KLML) laser was used for detecting the repetition rate (f_{ceo}), as indicated in Figs. 1 and 2. The repetition rate (f_{rep}) was then phase locked against an Agilent 8644A synthesizer (S1) with an 8 mHz instability at 0.2 s. The absolute frequency of the n-th mode (f_n) was found by beating f_n against the aforementioned CTS diode laser, and was stabilized by phase locking the beat note against the other Agilent 8644A synthesizer (S2). All the instruments' time bases in Fig. 1 were phase locked to a universal standard via the global position satellite (GPS) system to provide their long-term frequency accuracy. Under 4.8 W pump power at 532 nm, the maximum output power of the KLML laser was 440 mW at 820 ± 20 nm and 250 mW at 850 ± 20 nm, with 25 fs pulse width. As Fig. 1 shows, an notch-coated mirror at 820 ± 5 nm was employed immediately after laser output, with a small tilt angle, for conducting most of the laser power to the user while leaking out the 822 nm laser modes (~ 3 mW) for the f_n-stabilization. When pulse dispersion was considered, particularly for the experiments concerning the time-domain peak power [12], the notch-coated mirror was inadequate and could be replaced by one 90% reflectance laser output coupler (OC) with small tilt angle. The resultant weakly chirped 29 fs pulse is presented in the dash-line inset of Fig. 1, showing insignificant attrition of pulse peak power.

2.2 *Frequency stabilization*

The KLML laser in Fig. 1 was a z-type Ti:sapphire laser [15], which was modified from a commercially available model [16], as depicted in Fig. 2. All the mirror mounts were replaced by high stable mirror mounts [17] and the Ti:sapphire crystal (XTAL) was temperature controlled to within 0.01 °C variation by a pair of TE coolers to quietly dissipate the crystal heat. The repetition rate (f_{rep}) could be long-range tuned from 80 to 100 MHz by moving the output-coupler (OC) with a translational stage (TS), and could be finely tuned within several mHz by controlling the position of a piezo-mounted end mirror (EM, PZT1). The absolute frequency (f_n) of one certain mode of KLML could be long-range (45 MHz) scanned as well as be stabilized by horizon-

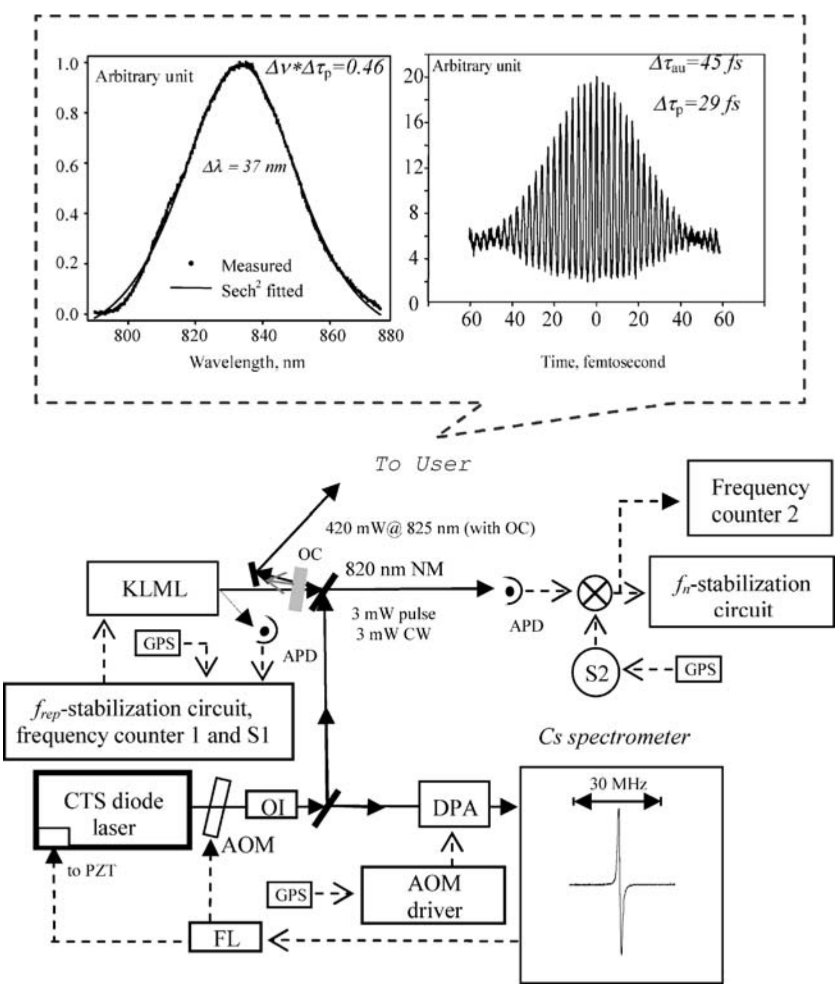

FIGURE 1 The block diagram of our frequency-stabilized Kerr-lens mode-locked laser system. KLML – Kerr-lens mode-locked femtosecond laser; S1,2 – frequency synthesizer 1,2; CTS – cesium two photon-stabilized; AOM – acousto-optic modulator; OI – optical isolator; DPA – double pass AOM; GPS – global position satellite; FL – feedback loop; f_{rep}: repetition rate; NM – 822 nm notch-coated mirror; OC – 90% reflectance output coupler; this component is optional in the case of minimmal pulse dispersion being required; APD – avalanche photo-diode; PL – pump laser; τ_{au} – measured by interferometric autocorrelator; τ_{p} – deduced pulse intensity width ($\mathrm{sech}^2(t)$ fit). The cesium spectrum was retrieved from DPA frequency dither, see text

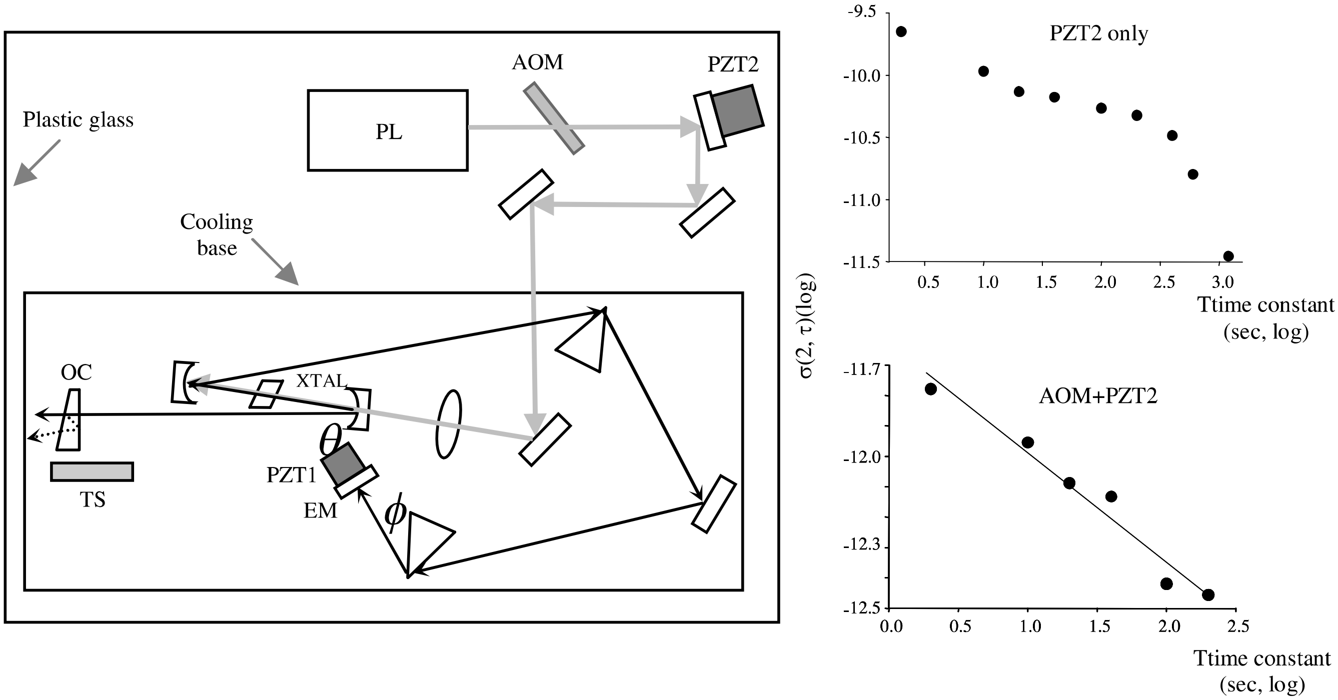

FIGURE 2 Block diagram for controlling the absolute frequency of our mode-locked laser. The scales are not proportional to the real situation. XTAL – Ti:sapphire crystal; OC – output coupler; TS – translational stage; EM – end-mirror; PL – 532 nm pump laser; PZT1,2 – piezo-electric transducer; *Grey line* stands for pump beam and *black line* stands for laser beam in cavity. *Right part* are Allan deviations recorded from the frequency counter 2 of Fig. 1; "PZT2 only" means that f_n was stabilized by PZT2 only; "AOM + PZT2" means that f_n was stabilized by both AOM and PZT2 with different loop transfer functions, respectively

tally shifting the pump beam using PZT2, with 0.0014 μm/V displacement. Since the voltage applied on PZT2 never exceeded 500 V, the maximum output beam shifting of the Ti:sapphire laser was estimated as being around 0.5 μm. This approach provides excellent orthogonal control between f_{rep}-stabilization and f_n-stabilization. For investigating the orthogonality, we scanned f_n over a half repetition rate by PZT2 and monitored the frequency fluctuation of the stabilized f_{rep} by frequency counter 1 in Fig. 1; no obvious interlock was found within 8 mHz uncertainty (at 0.2 s gate time). Moreover, comparing with the approach of controlling the pump power [9, 10] where the capture range of f_n-locking was around 2 MHz in our laser system, the approach of shifting pump beam provides one order of magnitude better capture range (35 MHz) thus frequency locking could routinely last for several hours. The principle of the orthogonal control could be comprehended by analyzing the variation of the repetition rate (f_{rep}). In other words, when we horizontally shifted the pump beam, a slight mode mismatching modified the self-phase modulation which was pulse-intensity-related, and that changed the round-trip carrier-envelop phase; while the change of repetition rate was not obvious for

$$f_{\mathrm{rep}} = \frac{V_{\mathrm{g}}}{L_{\mathrm{c}}} = \left(\frac{c}{n + \omega_{\mathrm{c}} \left(\frac{\mathrm{d}n}{\mathrm{d}\omega}\right)_{\omega_{\mathrm{c}}}} \right) / (L_0 + S(\cot\varphi - \cot\theta) - Dn_2(I_0 - I))\,, \qquad (1)$$

where V_{g} is the average group velocity inside the cavity [10]; $S\,(\geq 0)$ stands for the horizontal displacement of pump beam; L_{c} is the optical cavity length that equals to $L_0 + S(\cot\varphi - \cot\theta) - Dn_2(I_0 - I)$ where D is the XTAL length and φ, θ are indicated in Fig. 2; $n = n_0 + n_2 I$ is the average nonlinear index; I_0 is the laser intensity inside the cavity when PZT2 was not activated ($S = 0$) and I is that varied with S, that is, $I \equiv I_0 - \beta S$; Since $(\mathrm{d}n_2 D\omega)$ is relatively small ($\sim 10^{-38}$) [10], (1) could be approximated as

$$\begin{aligned} f_{\mathrm{rep}} = \frac{v_{\mathrm{g}}}{L_{\mathrm{c}}} &\sim \frac{c/(n_0' + n_2 I)}{L_0 + \alpha S} \sim \frac{c/(n_0' + n_2 I_0 - \beta S n_2)}{(L_0 + \alpha S)} \\ &\sim \frac{c}{(n_0' + n_2 I_0) L_0 + \left(\alpha \left(n_0' + n_2 I_0\right) - \beta n_2 L_0\right) S}\,, \end{aligned} \qquad (2)$$

where n_0' denotes $(n_0 + \omega_{\mathrm{c}}(\mathrm{d}n_0/\mathrm{d}\omega))_{\mathrm{average}}$; $\alpha \equiv (\cot\varphi - \cot\theta) Dn_2\beta$. Since $S \ll L_0$ and the value of α in our laser system could be adjusted so that $|\alpha(n_0 + n_2 I_0) - \beta n_2 L_0| \ll 1$, (2) is approximated as

$$f_{\mathrm{rep}} = \frac{c}{(n_0' + n_2 I_0) L_0} \sim \mathrm{const}\,.$$

The physical meaning is interpreted as follows. When mode mismatching is performed ($S \neq 0$), $n_0' + n_2 I$ in (2) will decrease since I decreases. That is, V_{g} increases. Meanwhile, $L_{\mathrm{c}}\ (= L_0 + \alpha S)$ increases so that compensates for most of the changing in f_{rep}. The right part of Fig. 2 presents the Allan deviations recorded from frequency counter 2 as in Fig. 1. When PZT2 was fed back only, the right upper panel of Fig. 2 shows 1 kHz instability at 1000 s sampling times. If the high frequency component of the error signal was further fed back to the AOM with different loop transfer function [18], one order of magnitude improvement could be achieved as shown in the bottom right of Fig. 2. Therefore, with PZT2 enlarging the frequency capture range and AOM for further stabilization, our

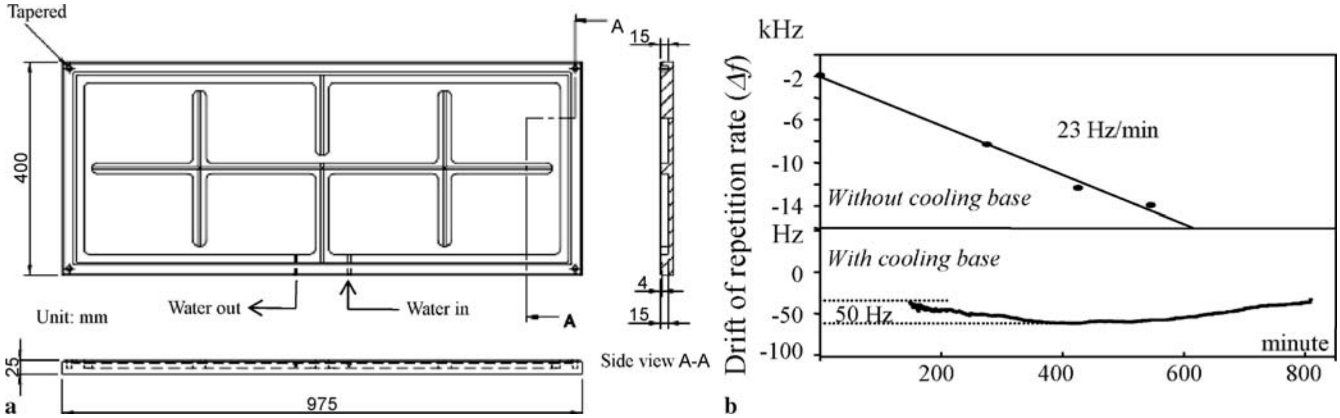

FIGURE 3 (**a**) Particular-designed cooling base which was installed beneath the comb laser. (**b**) The repetition-rate drifted 18 kHz during a 13 h period (*upper panel*), and was reduced two orders of magnitude after installing the cooling base (*lower panel*)

comb frequencies are easy to scan and stabilize. This fact also implies that people may use just one high frequency response component, such as the electric-optical modulator (EOM), to perform the beam shifting.

The f_{ceo} of our comb laser hence could be deduced from the fixed f_{rep} and the fixed f_n for

$$f_{\text{ceo}} = f_n - n \times f_{\text{rep}} . \tag{3}$$

Note that there are essential differences between the schematic of f_n-stabilization (in this paper) and f_{ceo}-stabilization (in the $1f$–$2f$ interferometer scheme). However, in the scheme of f_n-stabilization, the individual frequency f_m of the mode-locked laser was determined by $(m-n) \times f_{\text{rep}} + f_n$ while in the scheme of f_{ceo}-stabilization, f_m was determined by $m \times f_{\text{rep}} + f_{\text{ceo}}$. Since $m-n$ could be much smaller than m, the absolute frequency of f_m in our f_n-stabilization scheme was less sensitive to the fluctuations of f_{rep}, although f_{ceo} in the f_n-stabilization scheme is more sensitive to the fluctuation of f_{rep} than f_{ceo}-stabilization scheme. Therefore, stable f_{rep} is still important in any sort of frequency stabilization scheme. In general, every frequency-stabilized mode-locked laser will gradually lose the frequency locking due to the long-term drift of f_{rep}, especially when the room temperature is not rigorously regulated and the stretch length of PZT1 in Fig. 2 is limited. To keep a longer lifetime of frequency stabilization, we installed a particular-designed cooling base for controlling the cavity length in the long term, as depicted in Fig. 3a. The cooling base was connected to a chiller keeping the circulated water at $(19 \pm 0.05\,^\circ\text{C})$. Square-like partitions reduced the global turbulence during water flow. In Fig. 3b, the upper panel shows repetition rate over time in which no cooling base was installed; we recorded 18 kHz drift of repetition rate during 800 min ($\sim$ 13 h, extrapolated). When we installed the cooling base, a great improvement (two orders of magnitude) was achieved as shown in the bottom panel of Fig. 3b. The long term drift of repetition rate never exceed 50 Hz that was always within the capture range of PZT1.

2.3 *Scan of the absolute frequency*

As alluded to in Sect. 2.1, we implemented a double-pass AOM (DPA) system to retrieve the cesium spectrum and to move laser modes linearly and homogenously, as illustrated in Fig. 4.

For retrieving the cesium spectrum, we applied a 35 kHz frequency dither on the DPA system. The resultant first-derivative spectrum is presented in the "Cs spectrometer" part of Fig. 1, which was obtained with a 1 MHz-span frequency dither. This approach benefited from an un-modulated radiation (f_{DL}) for monitoring the absolute frequency of the mode-locked pulse. To investigate the frequency accuracy, we built up a second cesium two-photon stabilized diode laser system (CTS2) without double-pass AOM and directly modulated the diode current to retrieve the cesium spectrum. We alternated between the aforementioned two different sorts of modulations and monitored the beat note between two CTS lasers; no obvious discrepancy was observed within a 300 Hz uncertainty. Once the beat note frequency between the femtosecond laser and diode laser f_{b} $(= |f_n - f_{\text{DL}}|)$ was stabilized, we were able to linearly scan the DPA drive frequency to move all laser modes together. Consequently, laser modes could be

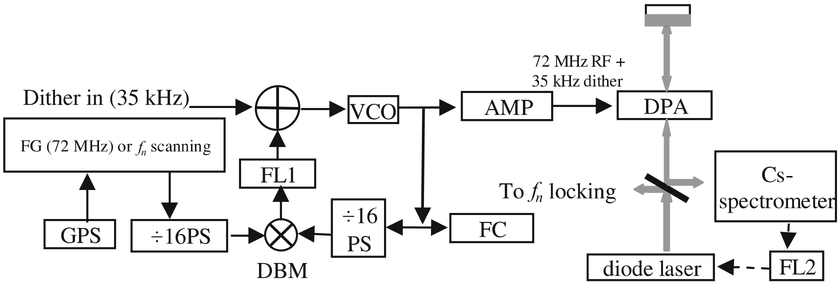

FIGURE 4 Frequency tuning, modulation and stabilization of double-pass AOM (DPA) system. FG – function generator which the output frequency could either be fixed at 72 MHz or be linearly scanned; f_n – absolute frequency of the nth comb mode; VCO – voltage controlled oscillator; AMP – amplifier; FC – frequency counter; PS – prescaler; DBM – double balance mixer; FL – feedback loop

Absolute frequency of f_n (MHz)[a]	364 507 094.417(15), linear scan range: $1/2 f_{\text{rep}}$
f_n instability (Δf_n)	200 Hz at 100 s
Estimated accuracy[b]	3000 Hz
User available comb power	440 mW at 822 nm
Repetition rate instability (Δf_{rep})	8 mHz at 0.2 s (f_{rep} tunable, 80–100 MHz)
ac stark shift of reference laser	$-18.9\,\text{Hz}/(\text{mW}/\text{mm}^2)$
Pressure shift of reference laser[c]	$-386\,\text{Hz}/°\text{C}$

[a] f_n stands for the nth mode that was phase locked to the reference laser, value adopted from [11] with DPA frequency equals to half of S1 frequency, see Fig. 1 and text;
[b] See text;
[c] Slope averaging from 68 to 84 °C cold finger temperature

TABLE 1 Specifications of our comb laser system

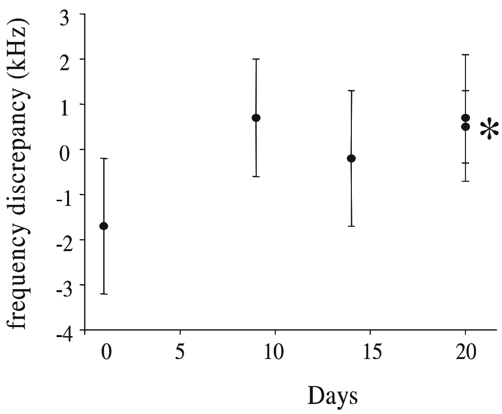

FIGURE 5 Frequency comparison between the comb laser and the other independent cesium-stabilized diode lasers. * – Data obtained from direct diode current dither while the other data were obtained from DPA dither

scanned over the entire laser emission spectra, with fixed repetition rate. When the DPA drive frequency was fixed to half of that in the S2 synthesizer in Fig. 1, the frequency of one particular mode (f_n) of mode-locked laser was exactly the same as the frequency of the cesium TPT-stabilized diode laser. In regard to the instability of the AOM drive frequency, we phase locked a voltage control oscillator (VCO) with an Agilent 33250A function generator (FG) as the AOM driving source, thus the instability of AOM drive frequency was reduced from $\Delta f_{\text{DPA}} = 2.6\,\text{kHz}$ (10 s) to $\Delta f_{\text{DPA}} = 0.8\,\text{mHz}$ (10 s).

3 Comb laser stability and accuracy

The frequency instability Δf_{comb} of our comb laser system hence was analyzed as:

$$\Delta f_{\text{comb}} = \Delta f_{\text{DL}} + \Delta f_{\text{b}} ,$$

where Δf_{DPA} is negligible as mentioned earlier, and Δf_{DL} stands for the frequency instability of CTS diode laser system, that is, $\Delta f_{\text{DL}} = 150\,\text{Hz}$ at 100 s, as had been proved in reference [14]; Δf_{b} stands for the frequency instability of f_{b} $(= |f_n - f_{\text{DL}}|)$, that is, $\Delta f_{\text{b}} = 140\,\text{Hz}$ at 100 s, as deduced from the bottom right part of Fig. 2. Therefore, the frequency instability of our comb laser (Δf_{comb}) was estimated as $\Delta f \sim 200\,\text{Hz}$ at 100 s. The spectral properties of the referring transition center were important in estimating the frequency accuracy of our comb laser. The power shift of atomic cesium $6S \rightarrow 8S$ hyperfine transition is $-18.9\,\text{Hz}/(\text{mW}/\text{mm}^2)$ and the pressure shift was smaller than 5 Hz if the cold finger temperature of cesium cell could be controlled to be smaller than 85 °C and within 0.01 °C accuracy. We estimated the accuracy of the comb frequency by the frequency comparison with the other CTS diode laser (CTS2) located on the other optical table with a different set of electronics. We turned off all lasers and the corresponding electronics after each measurement. Figure 5 shows the frequency discrepancy during 20 days of measurements which implied around 3 kHz accuracy. Uncertainty of the accuracy was attributed to the unstable room temperature during the data acquisition time period. In the accuracy measurements, two CTS diode lasers worked under the same cesium cell conditions, namely, $770\,\text{mW}/\text{mm}^2$ power density in the cell center (the waist) and 70 °C cold finger temperature. Table one summarizes the specifications of our comb laser system.

4 Conclusions

We have successfully built up a femtosecond Ti:sapphire comb laser based on a cesium-stabilized 822.5 nm diode laser. The available comb laser power was optimized and comb frequencies could be long range tuned with the repetition rate fixed, allowing for some applications of direct frequency comb spectroscopy (DFCS). We also demonstrated a novel idea of scanning and stabilizing the absolute frequency (f_n) by shifting the pump beam horizontally, without disturbing the repetition rate (f_{rep}) locking. Our comb laser system is a first step towards the experiments of direct frequency comb spectroscopy (DFCS). Since we are able to monitor and dither the absolute frequency of the comb laser, we are currently working on verifying the theory of reference [19] in which the non-relevance of absolute frequency in the experiment of coherent population trap (CPT), by pulse laser is detailed. To fulfill the experiment, the repetition rate should be always kept at the integer ratio of clock transition (9.192632 GHz) while the absolute frequencies of mode-locked laser were allowed to be scanned or dithered.

Though we have estimated the frequency accuracy of our comb laser, the comb laser in this report is not good enough for some ultrahigh-precision frequency measurements due to the imprecision of the absolute frequency in Table 1. Therefore, the other task for future work is to improve the absolute frequency measurement on the Cs-stabilized diode laser.

ACKNOWLEDGEMENTS We are grateful to Mr. Peter Chu for helping us design the cooling base of comb laser system; and the kind help of Dr. Barnes Keith in amending this article. This research is funded by the National Science Council: NSC 94-2112-M-001-022-MY3.

REFERENCES

1 S. Witte, R.T. Zinkstok, W. Ubachs, W. Hogervorst, K.S.E. Eikema, Science **307**, 400 (2005)
2 M.C. Stowe, F.C. Cruz, A. Marian, J. Ye, Phys. Rev. Lett. **96**, 153 001 (2006)
3 M.J. Thorpe, K.D. Moll, R.J. Jones, B. Safdi, J. Ye, Science **311**, 1595 (2006)
4 S.A. Diddams, L. Hollberg, V. Mbele, Nature **445**, 627 (2007)
5 H.R. Telle, G. Steinmeyer, A.E. Dunlop, J. Stenger, D.H. Sutter, U. Keller, Appl. Phys. B **69**, 327 (1999)
6 D.J. Jones, S.A. Diddams, J.K. Ranka, A. Stentz, R.S. Windeler, J.L. Hall, S.T. Cundiff, Science **288**, 635 (2000)
7 For example, J. Ye, L.S. Ma, J.L. Hall, Phys. Rev. Lett. **87**, 27 080 (2001)
8 T. Udem, J. Reichert, T.W. Hansch, M. Kourogi, Phys. Rev. A **62**, 031 801 (2000)
9 J. Stenger, H.R. Telle, Opt. Lett. **25**, 1553 (2000)
10 K.W. Holman, R.J. Jones, A. Marian, S.T. Condiff, J. Ye, Opt. Lett. **28**, 851 (2003)
11 P. Fendel, D. Bergeson, T. Udem, T.W. Hansch, Opt. Lett. **32**, 701 (2007)
12 For example, C. Gohle, T. Udem, M. Herrmann, J. Rouschenberger, R. Holzwarth, H.A. Schuesler, F. Krausz, T.W. Hansch, Nature **436**, 234 (2005)
13 R.J. Jones, J.-C. Diels, Phys. Rev. Lett. **86**, 3288 (2001)
14 C.-Y. Cheng, C.-M. Wu, G.-B. Liao, W.-Y. Cheng, Opt. Lett. **32**, 536 (2007)
15 G. Cerullo, S. Silvestri, V. Magni, L. Pallaro, Opt. Lett. **19**, 807 (1994)
16 Our laser was originally bought from Avesta Ltd. Model TiF-20
17 Lee's mounts, Linos Inc
18 The designs on the loop transfer functions for feeding back to PZT and AOM have been discussed in detail in: J.L. Hall, M.S. Tauburan, J. Ye, OSA Handbook **14**, 29 (1999)
19 L. Arissian, J.-C. Diels, Opt. Commun. **264**, 169 (2006)